



3D nonlinear ground motion simulation for postglacial sediments in Kinburn Basin

Amin Esmaeilzadeh¹, Dariush Motazedian²

¹ Ph.D. Candidate, Department of Earth Sciences, Carleton University - Ottawa, ON, Canada.

² Professor, Department of Earth Sciences, Carleton University - Ottawa, ON, Canada.

ABSTRACT

We used a finite difference (FD) modeling method, developed by Olsen-Day-Cui, to simulate nonlinear-viscoelastic basin effects, in the spectral frequency range of 0.1 to 1 Hz, in the Kinburn basin, Ottawa, Canada, with a very high (~20) shear-wave impedance contrast between bedrock and soil in comparison to typical contrasts of 3–5 in many other places. Cyclic nonlinear models, which mainly considered an elastoplastic behavior for soil deposits, determine the nonlinear stress-strain behavior of soil by following the actual stress-strain path during cyclic loading. In regular linear simulations, the shear modulus of soil is assumed constant in stress-strain relation. In proposed method, the shear modulus is defined as a function of strain and modified based on the strain level at each time step of simulation and for each element of soil. Detailed geophysical information was used to model the study basin and modulus reduction equation. The focal mechanism associated with the recorded May 17th, 2013 Ladysmith earthquake of M4.6 was used as a source while the magnitude was scaled to 7.5 in order to study the effects of nonlinearity. The nonlinear viscoelastic ground motions for the frequency range of 0.1 to 1 Hz were carried out for this simulation. Ground motion modeling in the Kinburn basin using a scaled Ladysmith earthquake event of Mw=7.5 showed the nonlinear relationship between stress and strain following Masing rules. The use of nonlinear-viscoelastic ground motion simulations reduced the amplitude of the horizontal component spectrum at low frequencies and the predicted PGA values compared to regular linear viscoelastic simulations.

Keywords: Finite difference (FD) modeling, nonlinear-viscoelastic basin effects, ground motion simulation

INTRODUCTION

There are three groups of parameters that influence ground motion for broadband frequency ground motion simulation in earthquake hazard analysis including: earthquake source effects (seismic moment, slip distribution, stress drop distribution, fault geometry, rupture velocity, etc.), path effects (distance, depth, crustal velocity structure, near source effects, etc.) and site effects (soil type, thickness and heterogeneity, 3D basin effect, etc.) [1-2].

The characteristics of the shaking at the ground surface (amplitude, frequency and duration) are mainly dependent on the materials through which the waves travel over the last few hundred meters (or less). Thus, local soil/site conditions play a key role in establishing the damage caused by seismic waves generated by earthquakes. In additions, there is a strong correlation between the level of earthquake ground shaking and some characteristics of the basin. Therefore, basin effects can be important controlling parameters that should be considered in the determination of ground motion amplification in an area [3-4-5-6-7-8].

In general, a basin seismic response is dependent on its geometry, the seismic impedance (shear wave velocity times density) contrast between sediments and bedrock, properties of sediments and shear modulus reduction of soil that describe soil nonlinear behavior and the characteristics of the seismic source (complexity and intensity). Some of these characteristics have 3D effects, due to their heterogeneities in geological units from the earthquake source to the soil in the basin [9]. Thus, for a more accurate simulation that allows for better understanding and assessment of the influence of different parameters that govern basin effects, 3D simulation methods need to be employed and improved. This is now possible due to the improvement in computer capabilities [10-11]. Three-dimensional basin modeling methods for linear soil have recently been performed by seismologists for eastern Canada using different programs (e.g., [12-13]); however, inclusion of a nonlinear source is still a challenge.

In this paper, the seismic response of the Kinburn basin in Ottawa, Canada was simulated to study the nonlinear soil behavior, using a newly developed routine to AWP-ODC (Anelastic Wave Propagation, developed by Olsen-Day-Cui program [14-15-16-17-18]). The main objective of this study is was to investigate the seismic amplification/de-amplification behaviour resulting from the basin and nonlinear soil characteristics.

STUDY STIE

The Kinburn basin is located in the Ottawa region as shown in Figure 1 (Vs30 map of the Ottawa region) [7-19]. The Kinburn basin is located 2.8 km southeast of the hamlet of Kinburn, Ontario, and is oriented in a northwest-southeast direction. This basin is one of the smaller interconnected basins in the region. The geotechnical and geological features of the Kinburn basin is unique: loose, postglacial sediments with very low shear wave velocities (< 200 m/s) overlying very firm bedrock with high shear wave velocities (> 2000 m/s) [2-19-20].

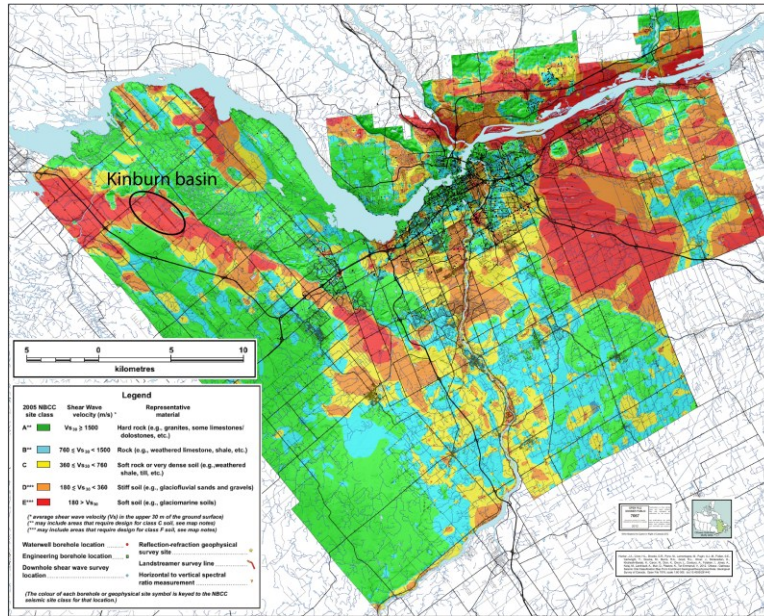


Figure 1. Vs30 map of the Ottawa region (Motazedian et al., 2011 and Hunter et al., 2012). The location of the Kinburn basin is indicated by the black circle.

In this research, the Kinburn basin depth (Figure 2) was modeled based on around 900 City of Ottawa water wells, 286 horizontal-to-vertical spectral ratio (HVSr) measurements [1-20], 2 high resolution Landstreamer seismic lines [21], and a GSC logged borehole [22]. The velocity profile of the Kinburn basin (Table 1) that was extracted from the borehole logging studies at a site near the deepest part of the basin was used to model the basin (Figure 2). The results of the simulation in this research are for the rock site (JSBS) and soil site (JSSS) in the Kinburn basin (Figure 2).

We used the Ladysmith earthquake, which occurred at 09:43 EDT (13:43 UTC) on 17 May 2013 with a measured Mw 4.7 (MN 5.2) happened 18 km northeast of Shawville in southwestern Quebec and 4 km from the small community of Ladysmith [23]. Although the Ladysmith earthquake is moderate in size (Mw 4.7, MN 5.2), it was one of the best-recorded earthquakes to occur in eastern Canada in recent years due to the density of the Canadian National Seismograph Network (CNSN) in western Quebec and eastern Ontario and the fortuitous deployment of several U.S. Transportable Array (USTA) stations in the region (Figure 3). The distance between the epicenter of the Ladysmith earthquake and the Kinburn basin is 43 km.

Published studies that calculate the focal mechanism of the Ladysmith earthquake use a wide variety of methods [24-25-26]. Our research on the simulations of the Ladysmith earthquake using these calculated focal mechanisms showed that the focal mechanism of Ma and Audet (2014) [24] (Table 2) more accurately predicted the earthquake ground motion within the basin; thus, the focal mechanism of Ma and Audet (2014) [24] was used in this study.

For Sake of simplicity, by using equation 1 the Ladysmith earthquake was scaled to Mw=7.5 to provide a large earthquake (strong incoming wave field) to investigate the nonlinear behavior of soil.

$$M_w = (\log M_0 - 9.1) / 1.5 \tag{1}$$

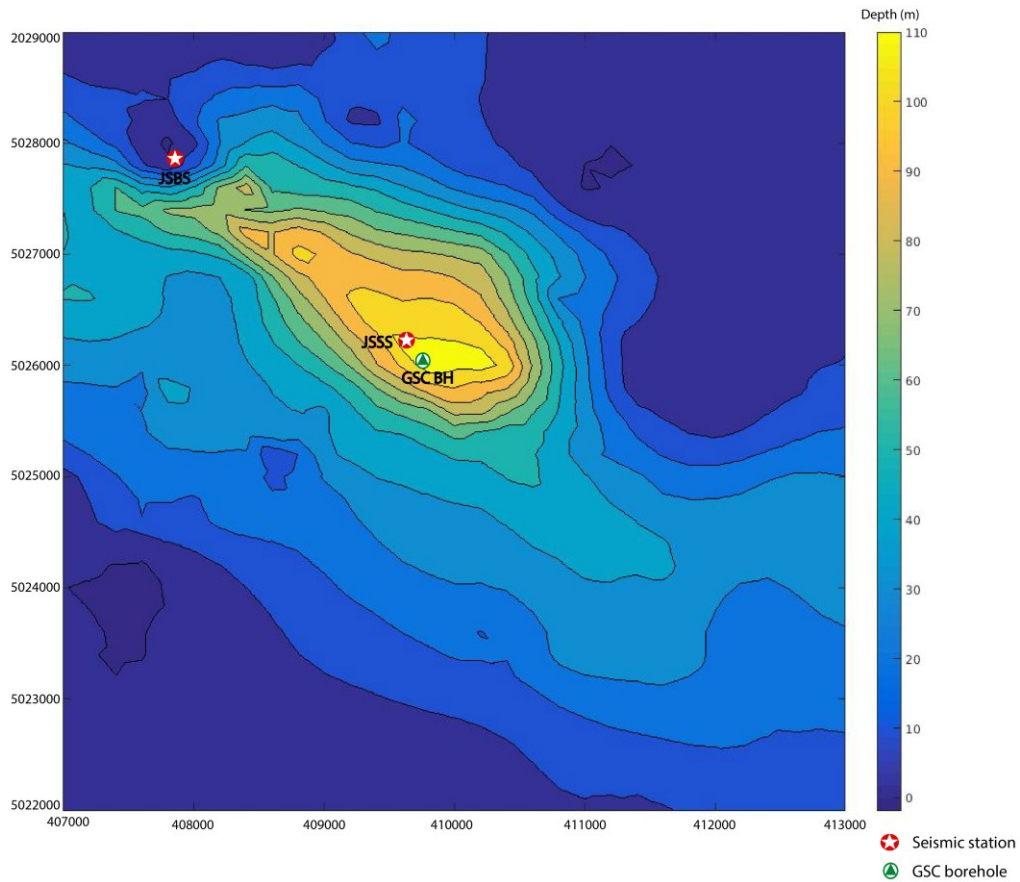


Figure 2. Kinburn basin depth model and locations of seismic stations (JSSS, JSBS) and GSC borehole (BH).

Table 1. Properties of the seismic velocity model (Burger et al., 1987; Eaton et al., 2006; Hunter et al., 2010; Crow et al., 2011; Bent et al., 2015).

| Type of material | Soil | Soil | Soil | Soil | Rock |
|------------------------------|------|-------|-------|--------|-------|
| Depth (m) | 0-25 | 25-50 | 50-75 | 75-100 | ----- |
| Vs (m/s) | 178 | 219 | 278 | 320 | 2783 |
| Vp (m/s) | 1380 | 1380 | 1380 | 1380 | 6200 |
| Density (kg/m ³) | 1600 | 1600 | 1600 | 1600 | 2650 |
| Qp | 185 | 185 | 185 | 185 | 1000 |
| Qs | 185 | 185 | 185 | 185 | 500 |

The Gaussian function (Equation 2) was used to model the evolution of the slip with time on the point source fault:

$$M(t) = \frac{M_0}{\sqrt{2\pi\sigma^2}} e^{-\frac{(t-\mu)^2}{2\sigma^2}} \quad (2)$$

where $M(t)$ is the seismic moment as a function of time, M_0 is the total seismic moment, μ is the mean of the distribution, and σ is the standard deviation of the distribution. The half duration of rupture used in the simulations is 0.6 seconds based on the proposed half duration for the Ladysmith earthquake used in the CMT method.

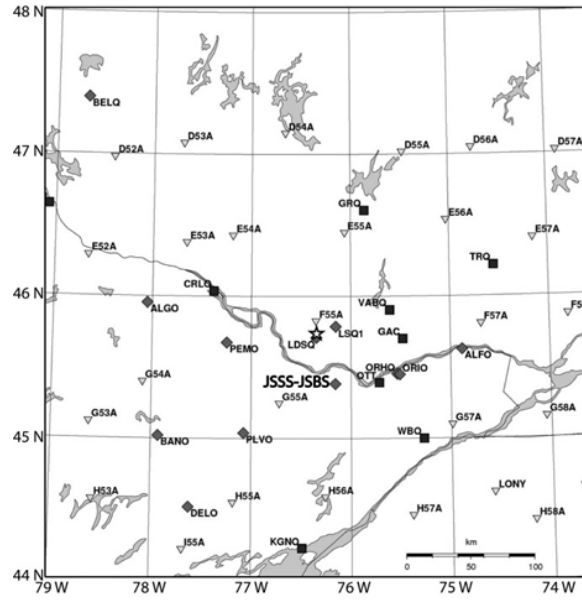


Figure 3. The open star shows the epicenter of the Ladysmith earthquake. Other symbols represent seismograph stations (diamonds: three-component broadband stations installed for research purposes; squares: permanent instruments of the Canadian National Seismograph Network; upside-down triangles: the U.S. Transportable Array stations; and JSSS-JSBS: the locations of the Kinburn basin array (Bent et al., 2015).

Table 2. The focal mechanism proposed for the Ladysmith earthquake by Ma and Pascal (2014)

| | | | |
|---------------------------|---------------|------------|-------------|
| Epicenter = 45.74, -76.34 | | | |
| Depth = 14.5 Km | | | |
| MW = 4.7 | | | |
| M0 = 1.32e+16 Nt-m | | | |
| | Strike | Dip | Slip |
| Plane 1 | 306 | 41 | 94 |
| Plane 2 | 122 | 50 | 87 |

PROPOSED NONLINEAR-VISCOELASTIC SIMULATION

There are several stress-strain relationship, such as Hook's law, the Duncan-Chang model or Hyperbolic model, and the (modified) Cam-Clay model, that can be used to formulate the relationship between stress (or stress increment) and strain (or strain increment) of soil. The AWP-ODC program solves a modified Hook's law of linear isotropic elasticity for stress-strain relationship (equation 3) to incorporate the effects of viscosity into time-stepped numerical simulations of wave propagation:

$$\sigma(t) = \text{Mu}[\varepsilon(t) - \sum_{i=1}^N \xi_i(t)] \quad (3)$$

where ξ_i , $i=1 \dots N$ are internal or memory variables that evolve with time, N is the number of relaxation terms in the approximation, Mu is the unrelaxed shear modulus, $\sigma(t)$ is stress as a function of time, and $\varepsilon(t)$ is strain as a function of time [27].

To implement nonlinear soil effects in AWP-ODC, we added a new subroutine to implement the shear modulus reduction curve at each time step, when the strain level exceeded the defined threshold strain (10^{-4}). In our modeling, we calculated a new shear modulus using a shear modulus reduction curve, Equation 4 proposed by Seed et al. (1970). Equation 4 shows the best fit to the average curve [28-29]:

$$\mathbf{G}/\mathbf{G}_{\max} = \frac{1}{[1+20\gamma(1+10^{(-10\gamma)})]} \quad (4)$$

VISCOELASTIC AND NONLINEAR-VISCOELASTIC GROUND MOTION SIMULATIONS OF THE KINBURN BASIN FOR THE SCALED LADYSMITH EARTHQUAKE MW=7.5, R=43 KM USING A POINT SOURCE MODEL

To consider the nonlinear soil effects for a large earthquake first, the ground motion from the scaled Ladysmith earthquake ($M_w=7.5$, $R=43$ km) was modeled for the Kinburn basin using the original viscoelastic simulation. Then, to demonstrate the impact of the introduced nonlinear soil behavior subroutine on the ground motion simulation, we modeled the nonlinear-viscoelastic ground motion of the Kinburn basin for the scaled Ladysmith earthquake ($M_w=7.5$, $R=43$ km) using the same velocity model and earthquake parameters that were used for the viscoelastic simulation. It should be noted that the nonlinear behavior was only modeled for the soil site.

Figure 4 shows the modulus reduction curve (left panel) and the strain-stress curve (right panel) for both viscoelastic simulation (called original) and newly implemented nonlinear-viscoelastic simulation (called modified) at the soil site (JSSS in Figure 3) for the $M_w=7.5$, $R=43$ km earthquake. Based on the calculated modulus reduction curves and stress-strain plots, the maximum nonlinear soil behavior happened in the X-Z component by factor of about 20%.

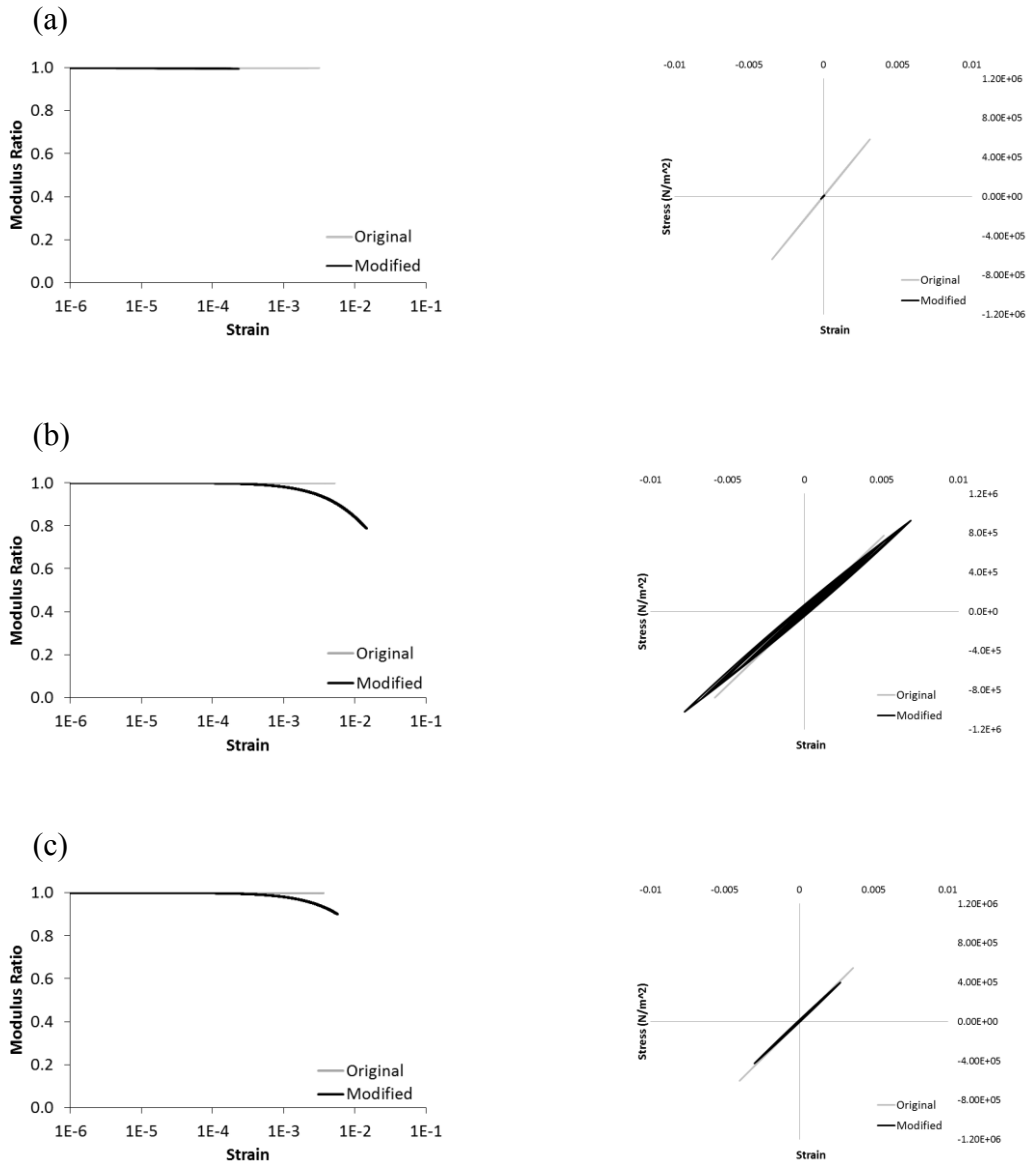


Figure 4. Modulus reduction and Stress-strain and curves of the a) X-Y component, b) X-Z component, and c) Y-Z component at the soil site for the viscoelastic (Original) and nonlinear-viscoelastic (Modified) simulations for $M_w=7.5$ ($R=43$ km, X = east-west, Y = north-south, Z = vertical)

The simulated acceleration time series for the soil site (Figure 5, left panel) showed that the PGA reduced from 0.88g in viscoelastic simulation to 0.65g in nonlinear-viscoelastic simulation while the PGA happened in E-W components for both

viscoelastic and nonlinear-viscoelastic simulations. Thus using nonlinear viscoelastic simulation reduced the predicted PGA by a factor of 28%.

The simulated acceleration Fourier spectrums at the soil site (Figure 5, right panel) shows that the viscoelastic simulation predicted an amplitude of acceleration Fourier spectrum of 1.6 m/s for the soil site which occurred at 0.94 Hz while the nonlinear-viscoelastic simulation predicted an amplitude of acceleration Fourier spectrum of 0.9 m/s for the soil site which happened at 0.79 Hz. Thus, using nonlinear-viscoelastic simulation reduced the predicted amplitude of acceleration Fourier spectrum by factor of 45%. Furthermore, using nonlinear-viscoelastic simulation shifted the frequency content of waves toward lower frequency.

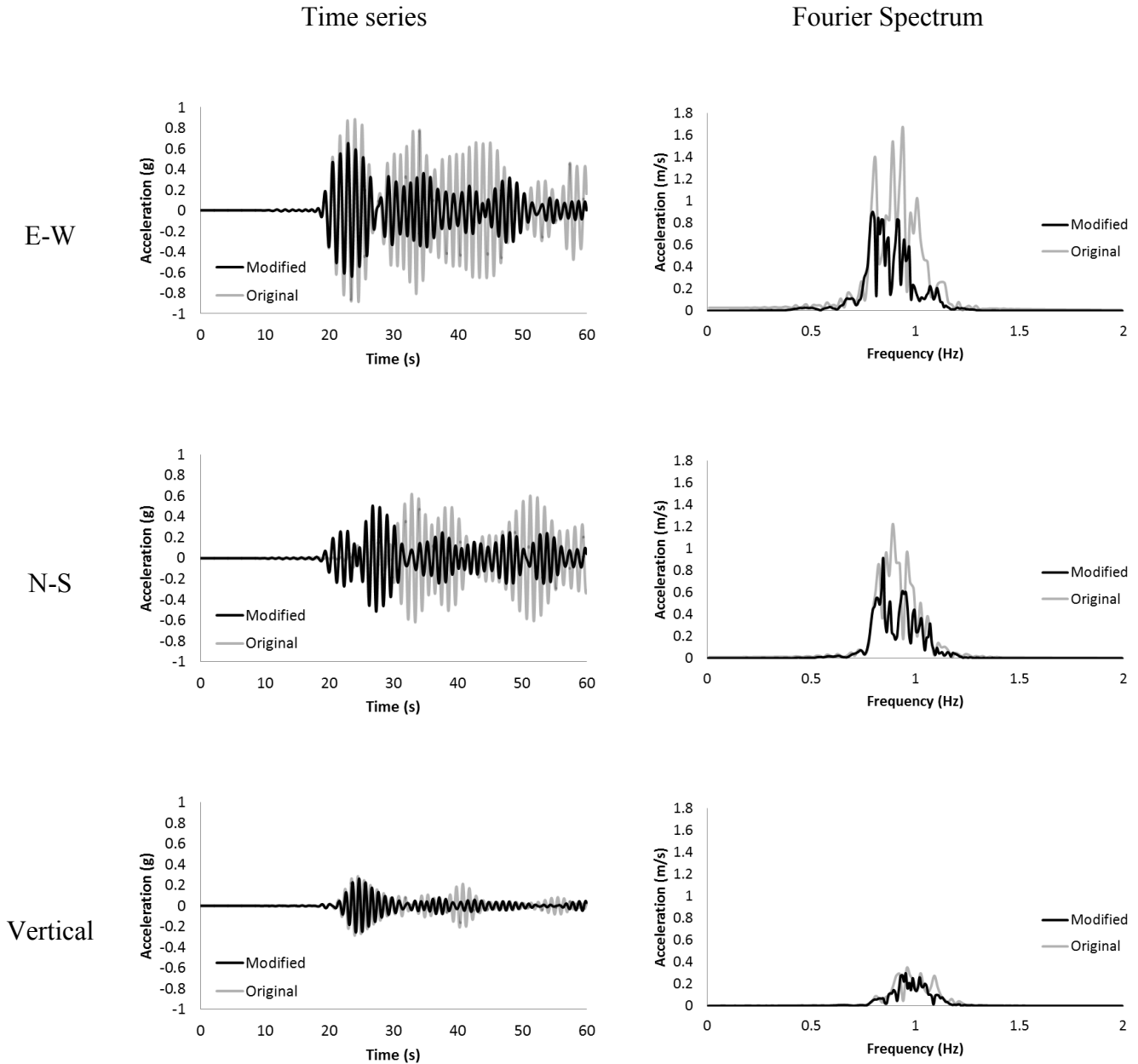


Figure 5. Acceleration time series and associated Fourier spectrums of the viscoelastic (Original) and nonlinear-viscoelastic (Modified) simulations for $M_w=7.5$ for the receiver at the soil site ($R=43$ km)

Using the ratio of the pseudo-spectral acceleration (PSA) of the soil site to the PSA of the rock site at 5% damping to calculate the amplification level in the soil site relative to the rock site (Figure 6) shows that the viscoelastic simulation

predicted which the maximum PSA ratio was equal to 19.5 at a frequency of 0.93 Hz and at N-S components while the nonlinear-viscoelastic simulation predicted that the maximum PSA ratio was equal to 14.5 at a frequency of 0.84 and at N-S component.

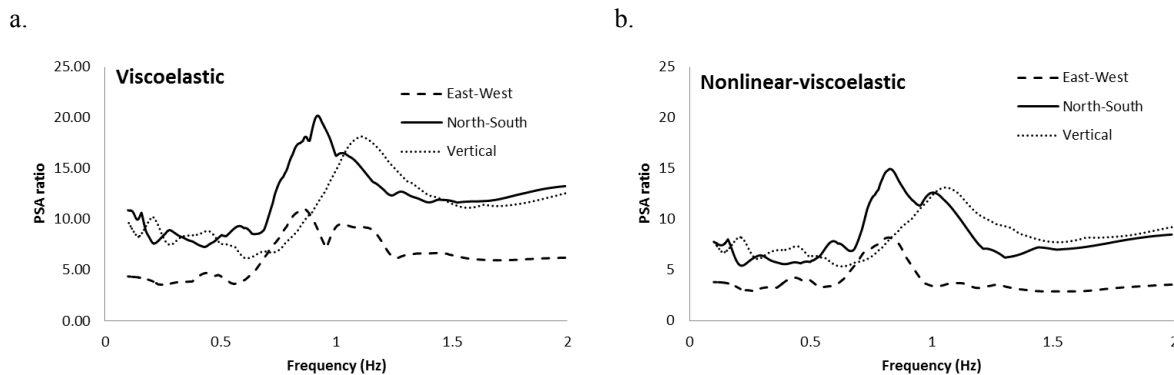


Figure 6. PSA ratio of soil site to rock site [$PSA(\text{soil site})/PSA(\text{rock site})$] for a. the viscoelastic simulation b. the Nonlinear-viscoelastic simulation

CONCLUSIONS

Using our newly introduced nonlinear-viscoelastic subroutine in our simulations of the ground motions of the Kinburn basin shows that when the strain level exceeds a defined yielding level (10^{-4}) during a large earthquake, the shear modulus of the soil in the basin are reduced compared to the shear modulus obtained using the original program. In our nonlinear-viscoelastic simulation, the PGA and the amplitude of acceleration Fourier spectrum of the soil site were lower (by factor of 27% and 45% respectively) relative to the PGA and the amplitude of acceleration Fourier spectrum of the soil site in the viscoelastic modeling. Furthermore, using nonlinear-viscoelastic simulation shifted the frequency content of waves toward lower frequency. Also, using the PSA ratio of soil site to rock site to predict the amplification that happened in the soil site shows that the predicted amplification of nonlinear-viscoelastic simulation is 26% smaller than the predicted amplification of the viscoelastic simulation. Further, the maximum PSA ratio of soil site to rock site happened at lower frequency in nonlinear-viscoelastic simulation compared to the frequency that the maximum PSA ratio happened in the viscoelastic simulation. Thus, ignoring nonlinear soil behavior in ground motion simulations can significantly increase the above-mentioned ground motion parameter values. However, using an accurate modulus reduction equation and a finite fault model for a large earthquake is necessary to have an accurate simulation as well.

ACKNOWLEDGMENTS

This research was supported by the Natural Sciences and Engineering Research Council of Canada under the Discovery Grant program and Collaborative Research and Development grants. This research used computational resources provided by the High Performance Computing Virtual Laboratory (HPCVL) and Calcul Québec, both under Compute Canada. We used the AWP-ODC [Anelastic Wave Propagation, developed by Olsen-Day-Cui] program package, and we would like to show our gratitude to Professor Kim Olsen for providing us with the package. We appreciate Dr. Daniel Roten's guidance in using the AWP-ODC program. Special gratitude is given to the Geological Survey of Canada for providing us with helpful comments, suggestions, and the necessary materials, including seismograms and geological information, for this research.

REFERENCES

- [1] Hunter, J. A., Burns, R. A., Good, R. L., Aylsworth, J. M., Pullan, S. E., Perret, D., & Douma, M. (2007). Borehole shear wave velocity measurements of Champlain Sea sediments in the Ottawa-Montreal region. Geological Survey of Canada, Open File #5345.
- [2] Hunter, J. A., Crow, H. L., Brooks, G. R., ... & Ter-Emmanuil, V. (2012). Ottawa-Gatineau seismic site classification map from combined geological/geophysical data. Geological Survey of Canada, Open File #7067.
- [3] Anderson, J. G., Bodin, P., Brune, J. N., Prince, J., Singh, S. K., Quaas, R., & Onate, M. (1986). Strong ground motion from the Michoacan, Mexico, earthquake. *Science*, 233(4768), 1043-1049.
- [4] Holzer, T. L. (1994). Loma Prieta damage largely attributed to enhanced ground shaking. *Eos, Transactions American Geophysical Union*, 75(26), 299-301.

- [5] Hisada, Y. & Yamamoto, S. (1996). One, two and three dimensional site effects in the sediment-filled basins. 11th World Conference on Earthquake Engineering, Acapulco, Mexico, Paper No. 2040.
- [6] Choi, Y. & Stewart, J. P. (2005). Nonlinear site amplification as a function of 30 m shear wave velocity. *Earthquake Spectra*, 21(1), 1-30.
- [7] Hunter, J. A. & Crow, H. L. (2012). *Shear Wave Velocity Measurement Guidelines for Canadian Seismic Site Characterization in Soil and Rock*. Geological Survey of Canada, Open File #7078.
- [8] Panzera, F. (2012). Approaches to earthquake scenarios validation using seismic site response. Ph.D. Thesis. University of Catania, Catania, Italy.
- [9] Kramer, S. L. (1996). *Geotechnical Earthquake Engineering*. Prentice Hall, Upper Saddle River, NJ, USA.
- [10] Yang, X. (2008). *Simulation of Seismic Real and Virtual Data Using the 3D Finite-Difference Technique and Representation Theorem*. Texas A&M University, TX, USA.
- [11] Gélis, C., Bonilla, F., & Peng-Cheng, L. (2011). Effect of Material Rheology When Modeling Wave Propagation in Complex Media: A 2D P-SV Case Study. 4th IASPEI / IAEE International Symposium, Santa Barbara, CA, USA.
- [12] Motazedian, D. and G.M. Atkinson (2005). "Stochastic Finite-Fault Modelling Based on a Dynamic Corner Frequency", *Bulletin of the Seismological Society of America*, 95, pp. 995-1010. [NSERC]. Download EXSIM_Beta (May, 26, 2009).
- [13] Atkinson, G. M. & Boore, D. M. (2007). Earthquake ground-motion prediction equations for Eastern North America. *Bulletin of the Seismological Society of America*, 97(3), 1032-1032.
- [14] Olsen, K. B. (1994). *Simulation of three-dimensional wave propagation in the Salt Lake Basin*. Ph.D. Thesis. Department of Geology and Geophysics, University of Utah, UT, USA.
- [15] Olsen, K. B., Archuleta, R. J., & Matarese, J. R. (1995). Three-dimensional simulation of a magnitude 7.75 earthquake on the San Andreas fault. *Science*, 270(5242), 1628-1632.
- [16] Olsen, K. B., Day, S. M., & Bradley, C. R. (2003). Estimation of Q for long-period (> 2 sec) waves in the Los Angeles basin. *Bulletin of the Seismological Society of America*, 93(2), 627-638.
- [17] Olsen, K. B., Day, S. M., Minster, J. B., Cui, Y., Chourasia, A., Faerman, M., ... & Jordan, T. (2006). Strong shaking in Los Angeles expected from southern San Andreas earthquake. *Geophysical Research Letters*, 33(7).
- [18] Cui, Y., Olsen, K., Chourasia, A., Moore, R., Maechling, P., & Jordan, T. (2009). The terashake computational platform for large-scale earthquake simulations. *Advances in Geocomputing*. Springer, Berlin, Heidelberg, 229-277.
- [19] Motazedian, D., Hunter, J. A., Pugin, A., Khaheshi Banab, K., & Crow, H. L. (2011). Development of a Vs30 (NEHRP) Map for the City of Ottawa, Ontario, Canada. *Canadian Geotechnical Engineering Journal*. doi:10.1139/T10-081.
- [20] Hunter, J. A., Crow, H. L., Brooks, G. R., Pyne, M., Motazedian, D., Lamontagne, M., ... & Burns, R. A. (2010). Seismic site classification and site period mapping in the Ottawa area using geophysical methods. Geological Survey of Canada, Open File #6273(1).
- [21] Pugin, A. M., Brewer, K., Cartwright, T., Pullan, S. E., Perret, D., Crow, H., & Hunter, J. A. (2013). Near surface S-wave seismic reflection profiling—new approaches and insights. *First Break*, 31(2), 49-60.
- [22] Medioli, B. E., Alpay, S., Crow, H. L., Cummings, D. I., Hinton, M. J., Knight, R. D., ... & Sharpe, D. R. (2012). Integrated data sets from a buried valley borehole, Champlain Sea basin, Kinburn, Ontario. *Current Research*, 3.
- [23] Basham, P. W., Weichert, D. H., & Berry, M. J. (1979). Regional assessment of seismic risk in eastern Canada. *Bulletin of the Seismological Society of America*, 69(5), 1567-1602.
- [24] Ma, S. & Audet, P. (2014). The 5.2 magnitude earthquake near Ladysmith, Quebec, 17 May 2013: implications for the seismotectonics of the Ottawa–Bonhechere Graben. *Canadian Journal of Earth Sciences*, 51(5), 439-451.
- [25] Atkinson, G. M., Assatourians, K., & Lamontagne, M. (2014). Characteristics of the 17 May 2013 M 4.5 Ladysmith, Quebec, Earthquake. *Seismological Research Letters*, 85(3), 755-762.
- [26] Bent, A. L., Lamontagne, M., Peci, V., Halchuk, S., Brooks, G. R., Motazedian, D., ... & Hayek, S. (2015). The 17 May 2013 M 4.6 Ladysmith, Quebec, Earthquake. *Seismological Research Letters*, 86(2A), 460-476.
- [27] Day, S. M. & Bradley, C. R. (2001). Memory-efficient simulation of anelastic wave propagation. *Bulletin of the Seismological Society of America*, 91(3), 520-531.
- [28] Seed, H. B. & Idriss, I. M. (1970). Soil moduli and damping factors for dynamic response analyses. Technical Report EERRC -70-10, University of California, Berkeley.
- [29] Rollins, K. M., Evans, M. D., Diehl, N. B., & III, W. D. D. (1998). Shear modulus and damping relationships for gravels. *Journal of Geotechnical and Geoenvironmental Engineering*, 124(5), 396-405.